

**EUR 4676 e**

COMMISSION OF THE EUROPEAN COMMUNITIES

ANALYSIS OF CRITICAL EXPERIMENTS ON  
THE SORA MOCKUP BY THE  $S_N$  METHOD

by

T. ASAOKA

1971



Joint Nuclear Research Centre  
Ispra Establishment - Italy  
Nuclear Study Division

## LEGAL NOTICE

This document was prepared under the sponsorship of the Commission of the European Communities.

Neither the Commission of the European Communities, its contractors nor any person acting on their behalf :

make any warranty or representation, express or implied, with respect to the accuracy, completeness, or usefulness of the information contained in this document, or that the use of any information, apparatus, method, or process disclosed in this document may not infringe privately owned rights ; or

assume any liability with respect to the use of, or for damages resulting from the use of any information, apparatus, method or process disclosed in this document.

This report is on sale at the addresses listed on cover page 4

at the price of F.Fr. 5.60 B.Fr. 50.— DM 3.70 It. Lire 620.— Fl. 3.60

When ordering, please quote the EUR number and the title, which are indicated on the cover of each report.

Printed by Vanmelle s.a., Ghent  
Luxembourg, July 1971

This document was reproduced on the basis of the best available copy.

**EUR 4676 e**

**ANALYSIS OF CRITICAL EXPERIMENTS ON THE SORA  
MOCKUP BY THE  $S_N$  METHOD** by T. ASAOKA

Commission of the European Communities  
Joint Nuclear Research Centre — Ispra Establishment (Italy)  
Nuclear Study Division  
Luxembourg, July 1971 — 36 Pages — 3 Figures — B.Fr. 50.—

This report summarizes the results of the analysis of the critical experiment for the pulsed fast reactor SORA by the use of the Carlson  $S_N$  method. Six-group two-dimensional  $S_4$  calculations of the reactivity for measured critical configurations confirm that the criticality of the SORA reactor can be predicted to within about  $\pm 1\%$  in the reactivity with the well known cross-sections tested for spherical critical assemblies. An analysis of measurements on the reactivity worth of a control rod or scatterer shows that the two-dimensional  $S_N$  code can be used to estimate the worth with a reasonable accuracy in the case where a precise treatment of the three-dimensional geometry is not essential.

---

**EUR 4676 e**

**ANALYSIS OF CRITICAL EXPERIMENTS ON THE SORA  
MOCKUP BY THE  $S_N$  METHOD** by T. ASAOKA

Commission of the European Communities  
Joint Nuclear Research Centre — Ispra Establishment (Italy)  
Nuclear Study Division  
Luxembourg, July 1971 — 36 Pages — 3 Figures — B.Fr. 50.—

This report summarizes the results of the analysis of the critical experiment for the pulsed fast reactor SORA by the use of the Carlson  $S_N$  method. Six-group two-dimensional  $S_4$  calculations of the reactivity for measured critical configurations confirm that the criticality of the SORA reactor can be predicted to within about  $\pm 1\%$  in the reactivity with the well known cross-sections tested for spherical critical assemblies. An analysis of measurements on the reactivity worth of a control rod or scatterer shows that the two-dimensional  $S_N$  code can be used to estimate the worth with a reasonable accuracy in the case where a precise treatment of the three-dimensional geometry is not essential.

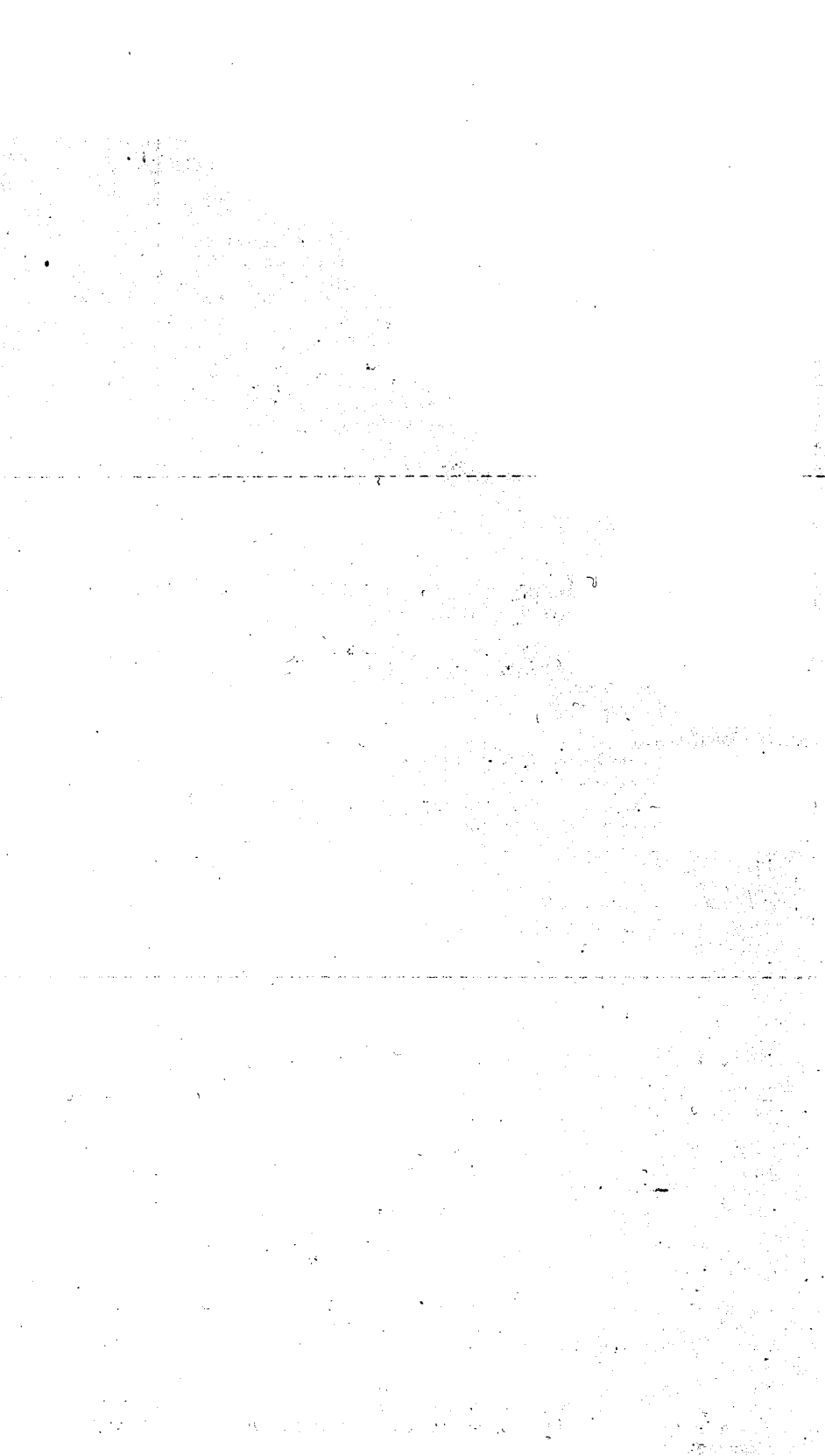
---

**EUR 4676 e**

**ANALYSIS OF CRITICAL EXPERIMENTS ON THE SORA  
MOCKUP BY THE  $S_N$  METHOD** by T. ASAOKA

Commission of the European Communities  
Joint Nuclear Research Centre — Ispra Establishment (Italy)  
Nuclear Study Division  
Luxembourg, July 1971 — 36 Pages — 3 Figures — B.Fr. 50.—

This report summarizes the results of the analysis of the critical experiment for the pulsed fast reactor SORA by the use of the Carlson  $S_N$  method. Six-group two-dimensional  $S_4$  calculations of the reactivity for measured critical configurations confirm that the criticality of the SORA reactor can be predicted to within about  $\pm 1\%$  in the reactivity with the well known cross-sections tested for spherical critical assemblies. An analysis of measurements on the reactivity worth of a control rod or scatterer shows that the two-dimensional  $S_N$  code can be used to estimate the worth with a reasonable accuracy in the case where a precise treatment of the three-dimensional geometry is not essential.



**EUR 4676 e**

COMMISSION OF THE EUROPEAN COMMUNITIES

ANALYSIS OF CRITICAL EXPERIMENTS ON  
THE SORA MOCKUP BY THE  $S_N$  METHOD

by

T. ASAOKA

1971



Joint Nuclear Research Centre  
Ispra Establishment - Italy  
Nuclear Study Division

## ABSTRACT

This report summarizes the results of the analysis of the critical experiment for the pulsed fast reactor SORA by the use of the Carlson  $S_N$  method. Six-group two-dimensional  $S_1$  calculations of the reactivity for measured critical configurations confirm that the criticality of the SORA reactor can be predicted to within about  $\pm 1\%$  in the reactivity with the well known cross-sections tested for spherical critical assemblies. An analysis of measurements on the reactivity worth of a control rod or scatterer shows that the two-dimensional  $S_1$  code can be used to estimate the worth with a reasonable accuracy in the case where a precise treatment of the three-dimensional geometry is not essential.

## KEYWORDS

SORA  
MOCKUP  
CRITICAL ASSEMBLIES  
REACTIVITY WORTHS  
CONTROL ELEMENTS  
CARLSON METHOD  
2-DIMENSIONAL CALCULATIONS  
RELIABILITY

## CONTENTS

1. Introduction	5
2. Preparation for $S_N$ Calculations	6
3. Design Calculations for the Mockup	9
4. Criticality Analysis	12
5. Reactivity Worths of Control Rods and Scatterers	14
6. Conclusion	20
References	21



ANALYSIS OF CRITICAL EXPERIMENTS ON THE SORA MOCKUP BY THE  $S_N$  METHOD \*)

1. Introduction

SORA is designed as a fast research reactor for pulsed neutron beam research<sup>1)2)3)</sup>. The theoretical reactor physics studies on the SORA reactor began at the beginning of 1962. As the reactor consists of a highly enriched small core surrounded by a very heterogeneous system of reflectors and scatterers, precise methods of solving the neutron transport equation were required. The Monte Carlo and Carlson  $S_N$  method were used for the study of all reactor statics problems.

The Monte Carlo programme (TIMOC) was developed to solve three-dimensional problems<sup>4)5)</sup>, particularly related to the value and the form of the reactivity pulse of the movable reflector which passes by the core-window to produce the pulses. Special geometry routines written for TIMOC allow a very detailed mockup of the reactor. The  $S_N$  method was mainly used for calculating problems which require a precise treatment of the mid-plane geometry. A number of problems can be solved by either the Monte Carlo or the  $S_N$  codes without making too serious assumptions. In these cases, the use of both methods enables a valuable double check to be made.

Even with the use of these advanced methods of calculation, it was decided that some experimental checks were necessary. A critical experiment programme for the SORA began at Oak Ridge National Laboratory in September 1965, under a cooperative agreement between EURATOM and USAEC, and most of the initially planned experiments were completed by early-1966<sup>6)</sup>.

The present report summarizes the results of analysis of the critical experiments performed by early-1967 with the  $S_N$  method. In Sec. 2, we discuss problems related to the use of  $S_N$  computer codes and multi-group cross-sections adopted for  $S_N$  calculations. Some topics with respect to design calculations for the SORA mockup are presented in Sec. 3. Following the presentation of the mockup geometry taken for the present calculation, the criticality analysis is discussed in Sec. 4. Finally the reactivity worth of a reflector or core component is evaluated in Sec. 5 and compared with the experimentally observed value.

---

\*) Manuscript received on March 11, 1971

## 2. Preparation for $S_N$ Calculations

The  $S_N$  codes<sup>7)8)</sup> which solve one and two-dimensional problems for a multi-energy group transport approximation were mainly used to calculate problems which require a precise geometrical treatment in the x-y plane but which are rather insensitive to the heterogeneity of the system in the z direction. For the solution of these problems, the 2DXY code<sup>8)</sup> has been adapted by introducing a set of axial bucklings to account for the finite extension of the system as well as the reflector savings in the z direction. Thus, an important problem is how to estimate the axial bucklings. The Boltzmann transport equation for stationary problems may be written, in a multi-group transport approximation, as follows:

$$\vec{\Omega} \cdot \text{grad} \Psi_i + \Sigma_{ti} \Psi_i = \frac{1}{4\pi} \sum_j (v f_j \Sigma_{fj} + \Sigma_{trj \rightarrow i}) \iint d\vec{\Omega}' \Psi_j(\vec{r}, \vec{\Omega}'), \quad (1)$$

where

$$\Psi_i(\vec{r}, \vec{\Omega}) = \int_{v_{i-1}}^{v_i} dv v N(\vec{r}, \vec{\Omega}, v),$$

$$\Sigma_{ti} = \Sigma_{ci} + \Sigma_{fi} + \sum_j \Sigma_{tri \rightarrow j}.$$

By adopting the cartesian coordinate and by integrating Eq. 1 over z, we get

$$\begin{aligned} & \vec{\Omega} \cdot \text{grad}_{x,y} \bar{\Psi}_i + \int dz \Omega_z \frac{\partial}{\partial z} \Psi_i + \Sigma_{ti} \bar{\Psi}_i \\ & = \frac{1}{4\pi} \sum_j (f_j v \Sigma_{fj} + \Sigma_{trj \rightarrow i}) \iint d\vec{\Omega}' \bar{\Psi}_j(x, y, \vec{\Omega}'), \end{aligned} \quad (2)$$

where

$$\bar{\Psi}_i(x, y, \vec{\Omega}) = \int dz \Psi_i(x, y, z, \vec{\Omega}).$$

Upon applying the diffusion theory approximation to the second term on the left hand side, by assuming that the behaviour of  $\Psi_i$  in the z direction is described by  $\cos(B_{zi}z)$ , Eq. 2 may be rewritten as

$$\begin{aligned} \vec{\Omega} \cdot \text{grad}_{x,y} \bar{\Psi}_i + (\Sigma_{ti} + D_i B_{zi}^2) \bar{\Psi}_i \\ = \frac{1}{4\pi} \sum_j (f_i \nu \Sigma_{fj} + \Sigma_{trj \rightarrow i}) \iint d\vec{\Omega}' \bar{\Psi}_j(x, y, \vec{\Omega}'), \end{aligned} \quad (3)$$

which can be solved by the use of the 2DXY code. The buckling values may be determined for each energy-group and space region from the axial flux distribution obtained by the use of the TDC code<sup>7)</sup> for the cylindricalized representation of the system.

Almost all the present calculations were performed with a 6-group  $S_4$  approximation.

The cross-sections used for the  $S_N$  calculations are based on the 18-group set of Los Alamos Scientific Laboratory<sup>9)10)11)</sup>. The group structure is shown in Table I. The following minor modifications were made to the 18-group cross-sections:

1. The first 6 group cross-sections for tungsten were replaced by the values from the 26-group set of Russian cross-sections<sup>12)</sup>. The original set was found to appreciably overestimate the effective multiplication factor in a calculation on an experimentally measured critical sphere surrounded by a tungsten alloy reflector.
2. The absorption and slowing down cross-sections of the first 2 groups for beryllium were modified to take into account the (n,2n) reaction adequately<sup>13)</sup>. Originally, the reaction was considered simply by a negative value of the absorption cross-section.
3. The transport cross-sections of the last 6 groups for hydrogen were modified to give the values in water<sup>14)</sup>.

For isotopes with resonance structure, the group cross-sections depend on the value of the potential cross-section per atom,  $\sigma_p$ . This effect

was taken into account only for U-235 and U-238 by using the approximate values of  $\sigma_f$ , 100 or  $\infty$  and 20, 200 or  $\infty$  barns respectively.

The collapsing of the 18-group cross-sections into 6 groups was performed with the help of the ZOT code<sup>15)</sup> using spectra obtained from a one-dimensional 18-group  $S_4$  calculation on a spherical representation of the SORA reactor. In Table I are shown the 6-group structure and the average velocities for each group calculated by using the spectra in the core, in the reflector and in the water scatterer, respectively.

The reduced 6-group cross-sections as well as the 18-group ones were tested by comparing the calculated values with experimental results. Table II shows the values of  $k_{eff}$  and Rossi- $\alpha$  at delayed critical for experimentally measured critical assemblies with ideal spherical geometry: Godiva<sup>16)17)</sup>, Topsy<sup>16)</sup>, ZPR-III-6F<sup>18)</sup>, Jezebel<sup>17)</sup> and Popsy<sup>17)</sup>. All these values were calculated with the 18-group  $S_4$  approximation.

The values of  $k_{eff}$ , which should be unity, never deviate by more than 1%. The Rossi- $\alpha$  at delayed critical was obtained from  $\beta_{eff}/l_{eff}$  where the effective delayed neutron fraction,  $\beta_{eff}$ , and the effective mean lifetime of prompt neutrons,  $l_{eff}$ , were estimated according to the formulae shown in the Reactor Handbook<sup>19)</sup>:

$$\beta_{eff} = \sum_{i=1}^6 \beta_i (W, f_i JN) / (W, f JN),$$

$$l_{eff} = (W, N) / (W, KN) = k_{eff} (W, N) / (W, f JN).$$

In Table II are shown also the results obtained from the use of the approximation of the integral  $(W, N)$  by  $(\int d\Omega W / 4\pi, \int d\Omega N / 4\pi)$ . These are given in parenthesis. All calculated values show, on the whole, a reasonable agreement with the experimental results though the Rossi- $\alpha$  is overestimated for Topsy due to the underestimate of  $l_{eff}^*$ .

---

\* We have recently recognized that in the final print of  $S_N$  codes the energy-group order of the adjoint flux is not restored to the correct one. The fact was first pointed out by E. Sartori of Ispra Establishment. As a result of restoring the correct group order, it becomes no more evident that  $S_N$  calculations underestimate the neutron lifetime of fast reactors by some 10 to 30%. K.D. Lathrop of Los Alamos Scientific Laboratory suggested that the

It is seen also that the above-mentioned approximation (neglecting the angular dependence) can be adopted for the reflected assemblies. All these calculations were repeated by using a 6-group  $S_4$  approximation. Only the difference between 6 and 18-group results was seen in the values of  $k_{\text{eff}}$ : the 6-group values are smaller by about 0.5%.

Tables III and IV show the values of  $k_{\text{eff}}$  obtained from 18-group or 6-group  $S_4$  calculations on experimentally measured critical spheres surrounded by a reflector of various materials [Table 7-13 of Ref. (20)]. The error in  $k_{\text{eff}}$  is at most 2%. The 6-group calculations give a very good approximation of the 18-group ones. In addition, one TDC test calculation was performed on a cylindrical critical core surrounded by a depleted uranium reflector with a thickness of 6.99 cm [the 93.2% enriched U core with 8.23 cm diameter and 70.6 cm height - see Table 7-18 of Ref. (20)]. The 6-group  $S_4$  calculation gave a value of  $k_{\text{eff}}$  1.009.

### 3. Design Calculations for the Mockup

The design of the mockup was based on  $S_N$  calculations. The aim in designing the mockup was to simulate the SORA reactor as well as we could.

To achieve an equivalent core, it was decided to use an iron block with holes into which U rods were inserted. This came from our estimate that about 45 vol% Fe would be required in the mockup core to simulate Mo in the U-10 w/o Mo fuel alloy, Incoloy canning of the fuel rod and NaK coolant of a reference core of the SORA reactor, the 93% enriched U rods occupying 65.6% of the total core volume.

Let  $a$  be the radius of the U rod and  $b$  the triangular lattice pitch (the distance between the centres of the rods arranged in a triangle lattice). Then, the ratio  $a/b$  is determined from the condition that the volume fraction of U is 0.656:

$$\pi a^2 / (\sqrt{3} b^2 / 2) = 0.656.$$

The core-window width  $d$  and core width  $t$  are given by (assuming the symmetric arrangement)

---

approximation generally adopted for evaluating the integral (W,N) might give an error in  $k_{\text{eff}}$ , by which the well-known underestimate would be compensated. The present calculation uses the delayed neutron data of G.P. Keepin given in "Delayed Fission Neutrons", Proceedings of a Panel, Vienna, 24-27 April, 1967.

$$d = b(\sqrt{3}m+1)/\sqrt{3}, \quad t = b(\sqrt{3}m+1),$$

where  $n+1$  rods are installed at the core-window and we have  $2m+1$  rows of rods within the core in the direction perpendicular to the window. The total number of rods which can be inserted in the core is given by

$$N = 2[(n+1) + (n+2) + \dots + (n+m)] + (n+m+1) = m(2n+m+2) + n+1 \quad \text{and the area is } A = \frac{\sqrt{3}}{2} b^2 N.$$

Table V shows some examples of the mockup core then proposed, which have a volume of about 5.5 l with the height 24 cm (expected to reach critical even in the worst case). The clearance between the U rod and the hole of Fe block was assumed to be 0.2 mm.

To examine how accurately the mockup core could simulate the real core, 6-group  $S_4$  calculations were carried out on sphericalized systems. The calculation was performed first on the sphericalized real reference core. Outside the homogenized core mixed with the volume for critical mass adjustment (where the fuel alloy was replaced by W) were placed 6 regions; 5 mm core vessel, 1 cm inner reflector, 1.1 cm homogenized region of control rods and moving reflector, 2 mm boron layer, 1 cm water layer and 22.5 cm outer reflector. The result showed that the critical radius of the homogenized core was 9.86 cm (4.02 l volume) and the critical mass of U-235 was 40.3 kg (43.4 kgU).

Then, fixing the core radius at this critical radius, the value of  $k_{\text{eff}}$  was evaluated for one of the mockup cores, with which the adjustment region were mixed in such a way that the ratio of the number of W rods to U rods was the same as that of the homogenized real core. The  $k_{\text{eff}}$  for this system was 0.99. The difference, 1%  $k_{\text{eff}}$  (we did not consider it serious at all), was not completely removed by adopting a thicker U rod or/and by reducing the clearance between the rod and the hole of Fe block. Even for the mockup core with 34.4 vol% Fe the  $k_{\text{eff}}$  was estimated to be about 0.995 according to the following empirical relations obtained from various one-dimensional  $S_4$  calculations on sphericalized SORA assemblies:

$$\frac{\Delta k_{\text{eff}}/k_{\text{eff}}}{\Delta V_c/V_c} (\text{reactivity change per core volume change}) = 0.27 \pm 0.03, \quad (4)$$

$$\text{Critical mass of U-235} \propto (\text{U-235 density in core})^{-(0.8 \pm 0.2)} \\ \times (\text{Total core density})^{-(0.5 \pm 0.2)}. \quad (5)$$

In addition to the criticality, one of the important quantities to be accurately simulated will be the neutron spectrum leaking out of the core because the reactivity worths of the moving reflector, control rods and so on depend on it. Eighteen-group one-dimensional  $S_4$  calculations performed on both the systems (in the mockup core the W adjustment rods were replaced by Fe) showed, on the whole, a good coincidence between the two leakage spectra, though for the mockup core the number of leakage neutrons belonging to 11th and 12th groups (22.6-3.06 eV) were larger by a factor of about 3 due to the absence of W (W adjustment rods in the real core were replaced later by Mo). The critical mass of the mockup core was thus estimated, from the relation (4), to be larger by 7% than the value of the real core for compensating the smaller  $k_{\text{eff}}$  by 1.9%. [The further 0.9% decrease in  $k_{\text{eff}}$  due to the replacement of W rods by Fe can be accurately predicted by using the empirical formulae (4) and (5).]

For estimating the critical mass of the real mockup with a height of 24 cm, we used, in addition to the relation (5), the shape factor (to convert the spherical into real critical mass)  $1.32 \pm 0.05$ . This value was obtained from a comparison between the critical mass of a sphericalized system and the result of a 2DXY calculation for the corresponding system. Combining the relation (5), the shape factor and the value of critical mass obtained from a one-dimensional  $S_4$  calculation, we got the following empirical relation:

$$\text{Critical mass of U-235 (kg)} = (53 \pm 3) (\rho_f/10)^{-(0.8 \pm 0.2)} (\rho_c/15)^{-(0.5 \pm 0.2)} \quad (6)$$

where  $\rho_f$  ( $g/cm^3$ ) and  $\rho_c$  ( $g/cm^3$ ) stand for the U-235 density in the core and the total core density respectively. This gave the critical mass of U-235  $49 \pm 5$  kg (corresponding to  $52 \pm 5$  kg U and  $4.2 \pm 0.4$  l core volume) for the mockup core without Fe dummy rods (not for the core mixed with the volume for the critical mass adjustment).

In fact, the critical mass for the nominal design (the Reference Assembly) of the mockup was 53 kg U-235 corresponding to 57 kg U or 85 U rods<sup>6</sup>, though the core composition was slightly different from that used for the estimation (see Table V).

#### 4. Criticality Analysis

Figure 1 shows the cylindricalized representation of the mockup with the nominal design configuration which was used for the TDC calculations. The core contains 85 fuel rods (see the last column of Table V); the radius and height are 7.890 cm and 24 cm respectively. The spatial mesh is indicated on the r and z axes (43 mesh points in each direction). The specification of the regions is given in Table VI (see also Fig. 2 and Table VII).

Figure 2 shows the mid-plane of the mockup adopted for the 2DXY calculations. Since the system is not completely symmetric about the y axis (as required for 2DXY), the calculations were performed separately on the control side (the left half of Fig. 2) and on the scatterer side (the right half). The spatial mesh is indicated on the x (43 mesh points on each side) and y (49 mesh points) axes. The region specification is given in Table VII.

For the first loading which became critical with 58 kg fuel on the 28th of September, 1965, a 6-group TDC calculation was performed to evaluate the axial bucklings. The cylindricalized representation for this system is shown in Fig. 1 by dotted lines. The core was composed of an inner part with 24 cm height and 6.05 cm radius and an outer part with 30 cm height and 7.63 cm outer radius. The region 3 contained only 54.8 vol%

Fe and the regions 4-6 consisted of 56.7% Fe and 43.3% Be to simulate the Fe control rods and Be moving reflector with 30 cm height. All other regions including the region 9 (beam holes) were filled with Fe.

From the resulting axial flux distributions, two sets of axial bucklings were estimated. The first set was chosen to represent the lower limit of the values (corresponding to the smallest possible axial leakage of neutrons) and the second one the upper limit. The latter is shown in Table VIII (no axial bucklings were applied to regions filled with air).

For these two sets of axial bucklings, 2DKY calculations were performed on the system with the first loading, which is shown by dotted lines on the left half of Fig.2. The regions 14 and 1 represent the core with 30 cm and 24 cm height respectively. The region 2 contained only 50.7 vol% Fe and the region 3 simulated the core-window composed of 5 mm Fe, 1 mm void, 7 mm Fe and 2 mm void<sup>\*</sup>. Region 8 was the Be moving reflector with 30 cm height. All other regions except for the regions 7 and 17 were filled with Fe and hence the system was symmetric about the y axis. The calculated values of  $k_{eff}$  were 1.018 and 0.998, respectively, which showed that the best axial bucklings were the maximum values determined by the use of the axial flux distributions.

This was verified by the result obtained from a 2DKY calculation on the system with the second loading which became critical with 51.5 kg fuel on the 4th of October, 1965. The configuration was the same as that for the first loading except that the core was composed of one region with 24 cm height and the region 2 was filled with Fe. The value of  $k_{eff}$  was found to be 0.997 using the second set of bucklings shown in Table VIII.

---

\* This void thickness turned out later to have been  $4 \pm 0.5$  mm. The increase  $2 \pm 0.5$  mm will decrease the value of  $k_{eff}$  by about 0.5%. In addition, as is shown at the end of Sec. 5, the reactivity worth of the moving reflector has been overestimated by about 1 dollar in the calculations. This must be the reason why the possible maximum values revealed themselves to be the best axial bucklings.

Another TDC calculation was performed on the nominal design configuration to determine the axial bucklings for the scatterers and the Be moving reflector with 24 cm height. The last 3 columns in Table VIII show the maximum values determined from the resulting axial flux distributions.

With the use of the axial bucklings (see the last row of Table VIII), 2DXY calculations were performed on the control rod side and scatterer side of the nominal design. The values of  $k_{\text{eff}}$  were found to be 0.996 and 0.979 respectively. The average value  $k_{\text{eff}} = 0.988$  agrees satisfactorily with the experimentally observed value 1.001, though the calculated value is smaller by 1.3%<sup>\*</sup>.

#### 5. Reactivity Worths of Control Rods and Scatterers

In order to estimate the reactivity worth of the Fe safety plug placed above the core, an additional TDC calculation was performed on the cylindrical representation of the nominal design in which the safety plug was removed completely. From the difference between the values of  $k_{\text{eff}}$  of the systems with and without the plug, the worth obtained was  $2.1 \pm 0.1\%$   $k_{\text{eff}}$ . This value is larger by nearly 40% than the experimentally measured value<sup>6)</sup>. In order to examine the effect of the region surrounding the safety plug, region 12 in Fig. 1, on the reactivity worth, further calculations were performed on the cylindrical system in which region 12 was composed of 50% Fe instead of 100% Fe. The worth decreased only slightly (about 5%).

---

\* In the geometry shown in Fig. 2, the void thickness next to the moving reflector is 5 mm, though the axial bucklings were determined for the system with the 2 mm void. Hence, if the axial bucklings were chosen for the system with the 5 mm void, the discrepancy 1.3%  $k_{\text{eff}}$  would be less than 0.8%  $k_{\text{eff}}$ .

The calculated worth of the Fe safety plug is thus  $2.0 \pm 0.2\%$   $k_{\text{eff}}$  ( $310 \pm 30$  ¢) and is overestimated by about 30% compared to the experimental value 235 cents. This overestimate may be due to the cylindricalizing approximation (the area of the cross section being the same as the actual one) by which especially the central part of the plug has too high a reactivity worth.

The reactivity worth of the Be control rod #1 or #5 (see Fig. 2) was calculated by replacing the Be by air with zero axial buckling; that is, under the assumption of no axial neutron streaming through this air channel. The resulting values obtained from the 2DXY calculations are  $1.18 \pm 0.08\%$   $k_{\text{eff}}$  ( $183 \pm 13$  ¢) for rod #1 and  $1.05 \pm 0.05\%$   $k_{\text{eff}}$  ( $163 \pm 8$  ¢) for rod #5 which agree rather well with the experimental values, 176-183 ¢ and 146-151 ¢ respectively. This agreement confirms the assumption that the axial neutron streaming through the air channel is negligible, due to the location near the boundary of the reactor system, compared to the effect caused by the change of a reflector thickness in the transversal direction.

The reactivity worth of the Fe piece #5b placed behind the control rod #5 was calculated in the same way as mentioned above. The calculated worth of  $0.071 \pm 0.001\%$   $k_{\text{eff}}$  or  $11.0 \pm 0.2$  ¢ compares well with the experimentally observed value 14.5 cents.

As concerns the control rod #2a, the reactivity worths of various materials were calculated for the two cases where a 1 or 2 cm Fe layer was placed between the rod and the core. The calculated values under the assumption of zero axial buckling for the voided region are summarized in Table IX. From these results together with the results shown in Table III, we can estimate that the axial neutron streaming gives an additional worth of about 30 ¢ for the case with the 2 cm Fe layer. For the other case with the 1 cm Fe layer, the additional worth will be nearly 40 ¢ because the ratio of this value to the 30 ¢ is about the same as that of the experimentally observed worths for both cases (the ratio is also about the same as that of the squared values of the average fluxes over the air channel for both cases - see Eq. 12). These values for the axial streaming effect on the reactivity seem to be reasonable because the deviation of

the modified reactivity worth from the experimental value is less than 10% for all cases except for the Fe rod. The reason why the worth of the Fe rod is overestimated (contrary to the fact that the  $k_{eff}$  are underestimated for Fe reflected spheres shown in Table III) can be seen from Table III where the 2% underestimate in the  $k_{eff}$  for the 5.08 cm Fe reflected sphere goes down to 1% for the 10.16 cm Fe reflected sphere.

The reactivity worth of scatterer #4 was calculated by replacing the material by air with zero axial buckling. The polyethylene core has a calculated reactivity worth of  $23 \pm 8 \%$  and the entire scatterer including the container has a worth of  $95 \pm 8 \%$ . The agreement of these values with the experimental results, 8.0 % and 67.1 % respectively, is rather good which partially validates the assumption of zero axial buckling in the voided region. This will come from the fact that the scatterer is located outside the core with big beam holes behind it.

For estimating the reactivity worth of a control rod as a function of the withdrawal distance, one-group first order perturbation theory was used. Let  $k(d)$  be the effective multiplication factor for the system where the control rod is withdrawn by the distance  $d$ . Then the reactivity worth of the control rod may be written, in first order perturbation theory, as<sup>19)</sup>

$$\rho(d) = 1 - \frac{k(\infty)}{k(d)} \approx \frac{(W, \delta KN)}{(W, KN)} - \frac{(W, f \delta JN)}{(W, fJN)}, \quad (7)$$

where  $\delta K$  and  $\delta J$  stand for the changes in the operators  $K$  and  $J$  due to the withdrawal from  $d$  to  $\infty$ . Since  $\delta J = 0$  in the present case, the  $\rho(d)$  is proportional to  $(W, \delta KN)$ .

Assuming that  $\frac{\partial \psi_i}{\partial x} = \frac{\partial \psi_i}{\partial y} = 0$  (see Eq. 1) in the region of the control rod and applying diffusion theory to the term  $\Omega_R \frac{\partial \psi_i}{\partial z}$ , Eq. 1 may give

$$\delta KN_i = \delta (D_i B_{Ri}^2 + \Sigma_{ti}) \phi_i - \sum_j \delta \Sigma_{trj \rightarrow i} \phi_j, \quad (8)$$

where 
$$\phi_i(\mathbf{z}) = \iint_{\text{control rod}} dx dy \iint d\vec{\Omega}' \psi_i(x, y, \mathbf{z}, \vec{\Omega}').$$

Hence, in a one-group model,

$$\rho(d) \propto \delta(DB_{\mathbf{z}}^2 + \Sigma_a) \int_{\text{control rod}} d\mathbf{z} \phi^*(\mathbf{z}) \phi(\mathbf{z}),$$

or 
$$\rho(d)/\rho(0) = \frac{\int_{-h+d}^{h+d} d\mathbf{z} \phi^*(\mathbf{z}) \phi(\mathbf{z})}{\int_{-h}^h d\mathbf{z} \phi^*(\mathbf{z}) \phi(\mathbf{z})}, \quad (9)$$

where  $2h$  is the rod length.

Since the third energy-group is the most important, the evaluation of Eq. 9 was performed with the regular and adjoint flux belonging to the third group obtained from the TDC calculation on the geometry shown in Fig. 1. The result for the Be control rod #5 is shown in Fig. 3 where the total worth  $\rho(0)$  has been normalized to 150  $\epsilon$  (the calculated value is  $163 \pm 8 \epsilon$ ). It is seen that the calculated result agrees well with the experimental curve.

The reactivity worth of the entire scatterer #4 is shown in Fig. 3 as a function of the withdrawal distance, the total worth being normalized to 67  $\epsilon$ . The calculated results agree reasonably with the experimental values. The slight overestimation seen in the middle of the withdrawal will be due to the fact that the flux in the scatterer channel around the mid-place of the reactor (the lower end of the scatterer withdrawn) is perturbed to become lower than the unperturbed value.

According to Eq. 7, the reactivity worth of a rod inserted in the core is written as

$$\rho \simeq (W, \delta(k_{\text{eff}}K - fJ)N) / (W, fJN), \quad (10)$$

where  $\delta$  stands for the change caused by replacing a rod by air. Inside the core, especially in the central part, one can assume that  $\frac{\partial \psi_i}{\partial x} = \frac{\partial \psi_i}{\partial y} = 0$  and hence it follows from Eq. 3 that

$$\begin{aligned} \delta(k_{eff}K - fJ)N_i &= k_{eff} \delta(\Sigma_{ti} + D_i B_{zi}^2) \phi_i \\ &\quad - k_{eff} \sum_j \delta \Sigma_{trj \rightarrow i} \phi_j - f_i \sum_j \delta(\nu Z_f)_j \phi_j, \end{aligned} \quad (11)$$

where

$$\phi_i(x, y) = \iint d\vec{\Omega} \bar{\psi}_i(x, y, \vec{\Omega}) = \iint d\vec{\Omega} \int dz \psi_i(x, y, z, \vec{\Omega}).$$

In a one-group model, Eqs. 10 and 11 give

$$\rho \approx \frac{\iint_{rod} dx dy \phi^* \delta(k_{eff}(\Sigma_a + DB_z^2) - \nu Z_f) \phi}{\iint_{core} dx dy \phi^* \nu Z_f \phi} \quad (12)$$

The calculations were performed first on a U rod at various positions by the use of the regular and adjoint fluxes of neutrons belonging to the third energy-group (the dominant group in the core spectrum), with the assumption that  $B_z^2 = 0$  for the voided channel ( $B_z^2 = 0.0085 \text{ cm}^{-2}$  for the U rod - see Table VIII). The results are given in Table X where the rod location indicated by a number in the first column is shown in Fig. 2. The results for the rods located on the y axis in Fig. 2 have been obtained by taking the average over the values on the control rod and the scatterer sides. As is seen in Table X, all the calculated values are smaller by about 30 % than the experimental results. The difference must come mainly from the axial neutron streaming through the voided channel and partly, especially for the rods located near the core boundary, from the transversal neutron leakage through the channel. Hence, the difference between the calculated and experimentally observed values must be the additional worth of the rod (the value being given in the fourth column of Table X).

Next, the reactivity worths of Mo, Fe and Ti rods were obtained by taking into account the leakage effect through the voided channel as mentioned above and by fixing the value of  $B_p^2$  for the rods to be  $0.0085 \text{ cm}^{-2}$ . As shown in Table X, for the Mo rod, the calculated values (with the correction) agree nicely with the experimental results. For the Fe and Ti rods, the calculations underestimate the worths of rods located in the central part of the core and overestimate those of rods located near the core boundary. The underestimation may be due to the fact that the value of  $B_p^2$  for the rods should be smaller than that for the U or Mo rod because of the axial neutron streaming through the rods (the values of  $\Sigma_{tr}$  for Fe and Ti are smaller by a factor of about 2 than those for Mo and U). On the other hand, the overestimation for the rods located near the core boundary may be due to the influence of neutrons belonging to the fourth energy-group. Near the core boundary, especially near the scatterer #3 where the rod 5 is placed, the fourth group has an influence on the criticality while in the central part of the core the influence is negligible. This means that the calculated worth of the U rod located near the core boundary has been underestimated and hence the leakage effect through the voided channel has been overestimated. In addition to this, the overestimation of the reactivity worths of Fe and Ti rods may come from the fact that the transversal neutron leakage through the rods with relatively small values of  $\Sigma_{tr}$  becomes of importance near the core boundary.

The reactivity worths of the Be moving reflector with various widths were calculated by replacing the moving reflector (region 8 in Fig. 2 where the width is 11 cm) and the arm (region 9) by air. In the every case where the width was more than 11 cm, the region 8 shown in Fig. 2 was extended sideways ignoring the slight curvature of the front face. In Table XI are shown the results which were obtained by averaging the values on both sides, the worth on the control rod side being higher only by 1-2% than that on the scatterer side. As is seen in Table XI, all the calculated worths are overestimated by about 1 dollar compared to the experimental values\*. This will come mainly from homogenizing the window region (region 3 in Fig. 2) and the use of the transport approximation with isotropic scattering.

---

\* see next page

## 6. Conclusion

The analysis of the critical experiments by the use of the  $S_N$  method has shown that the effective multiplication factor of a fast reactor with a compact core surrounded by a heterogeneous reflector can be predicted to within about  $\pm 1\%$ . Two-dimensional  $S_N$  codes in the transport approximation are used for the calculation by adopting the 6-group cross-sections collapsed from the 18-group set of the Los Alamos Scientific Laboratory. This reduction in the number of groups is accomplished with the help of the spectra obtained from a one-dimensional 18-group  $S_4$  calculation on a spherical representation of the reactor. The 2DXY code is applied to the mid-plane geometry of the reactor using the axial buckling determined (for each energy-group and space region) from the flux distribution calculated by the use of the TDC code in a cylindrical representation of the system.

The reactivity worth of a reflector component can be evaluated with reasonable accuracy from the 2DXY calculations in the case where the axial neutron streaming through the voided region is unimportant. In the case where the axial streaming plays an important role, the measured worth is used for an estimation of the streaming effect on the reactivity. By the use of this value, we can estimate the reactivity worth of a reflector or core component with a material different from the measured case. However, for dealing with problems which require a precise treatment of the three-dimensional geometry of the reactor, the Monte Carlo method is more suited than the  $S_N$  approximation.

A better agreement between the calculated and measured reactivity worths of a control rod or scatterer may be achieved by correcting the cross-sections. We, however, think that the present accuracy in the cross-section is comparable to that in the calculation method and, on the whole, enough for a design calculation.

---

\* The Monte Carlo code has given an accurate reactivity worth of the moving reflector. The reactivity pulse shape of the moving reflector as a function of its position was calculated only by the Monte Carlo method and compared with the experimental result<sup>4)</sup>.

References

- (1) V. Raievski et al., "The Pulsed Fast Reactor as a Source for Pulsed Neutron Experiments", IAEA Symp. Pulsed Neutron Research, Vol. II, 553, Karlsruhe (1965).
- (2) J.A. Larrimore, R. Haas, K. Giegerich, V. Raievski and W. Kley, "The SORA Reactor; Design Status Report", AEC-ENEA Seminar Intense Neutron Sources, Sante Fé (1966).
- (3) J.A. Larrimore, R. Haas, K. Giegerich, V. Raievski and W. Kley, "SORA", ANS Symp. Fast Burst Reactors, Albuquerque (1969).
- (4) H. Rief and H. Kschwendt, "Reactor Analysis by Monte Carlo", Nucl. Sci. Engng. 30, 395-418 (1967).
- (5) H. Rief, H. Kschwendt and R. Jaarsma, "Reactivity Calculations for a Periodically Pulsed Fast Reactor by the TIMOC Code", Proc. Int'l Conf. Research Reactor Utilization and Reactor Mathematics, Vol. I, 488, Mexico City (1967).
- (6) G. Kistner and J.T. Mihalczo, "Critical Experiments for the Repetitively Pulsed Reactor SORA", Nucl. Sci. Engng. 35, 27-44 (1969).
- (7) B. Carlson, C. Lee and J. Worlton, "The DSN and TDC Neutron Transport Codes", LAMS-2346, Los Alamos Scientific Laboratory (1960).
- (8) J. Bengston, S.T. Perkins, T.W. Sheheen and D.W. Thompson, "2DXY, Two Dimensional, Cartesian Coordinate  $S_n$  Transport Calculation", AGN TM-392, Aerojet-General Nucleonics (1961).
- (9) C.B. Mills, "Physics of Intermediate Reactors", LAMS-2288, Los Alamos Scientific Laboratory (1959).
- (10) W.H. Roach, "Computational Survey of Idealized Fast Breeder Reactors", Nucl. Sci. Engng., 8, 621-651 (1960).
- (11) G.E. Hansen and W.H. Roach, "Six and Sixteen Group Cross Sections for Fast and Intermediate Critical Assemblies", LAMS-2543, Los Alamos Scientific Laboratory (1961).

- (12) L.P. Abagjan et al., "Gruppenkonstanten schneller und intermediärer Neutronen für die Berechnung von Kernreaktoren", L. Neander transl., KFK-tr-144, Karlsruhe (1964).
- (13) B.R.S. Buckingham, K. Parker and E.D. Pendlebury, "Neutron Cross-Sections of Selected Elements and Isotopes for Use in Neutronics Calculations in the Energy Range 0.025 eV-15 MeV", AWRE Report No. O-28/60, Atomic Weapons Research Establishment (1960).
- (14) D.J. Hughes and R.B. Schwartz, "Neutron Cross Sections", BNL-325, Second Ed., Brookhaven National Laboratory (1958).
- (15) R.S. Cooper, "A Code for Reducing Many-Group Cross Sections to Few Groups", LAMS-2801, Los Alamos Scientific Laboratory (1963).
- (16) G.E. Hansen, "Properties of Elementary Fast-Neutron Critical Assemblies", Proc. Geneva Conf., Vol. 12, 84-88, P/592 (1958).
- (17) G.A. Jarvis et al., "Two Plutonium-Metal Critical Assemblies", Nucl. Sci. Engng. 8, 525-531 (1960).
- (18) J.K. Long et al., "Fast Neutron Power Reactor Studies with ZPR-III", Progress in Nuclear Energy, Series II, Reactors, Vol. 2, H.R. Mck. Hyder Ed., 201-246, Pergamon Press (1961).
- (19) G. Goertzel, Reactor Handbook, Vol. 1, Physics, AECD-3645, Chap. 1.6, United States Atomic Energy Commission (1955).
- (20) Argonne National Laboratory, Reactor Physics Constants, ANL-5800, Second Ed., Sec. 7, United States Atomic Energy Commission (1963).

TABLE I Eighteen and Six Energy-Group Structures used for  $S_N$  Calculations

18-group			6-group			
	Upper limit of energy range	Average velocity ( $10^8$ cm/sec)		Average velocity ( $10^8$ cm/sec) obtained from spectrum		
				in core	in reflector	in water scatterer
1	10 MeV	28.5	1	28.5	28.5	28.5
2	3	19.9	2	17.5	16.6	17.1
3	1.4	14.7				
4	0.9	11.0	3	8.42	7.78	8.10
5	0.4	6.7				
6	0.1	2.70	4	2.61	1.84	1.06
7	17 keV	1.237				
8	3	0.5071				
9	0.454	0.1866	5	0.161	0.110	0.0367
10	61.44 eV	0.0854				
11	22.6	0.0518				
12	8.315	0.0314				
13	3.059	0.0191				
14	1.126	0.0116				
15	0.414	0.00701	6	0.0070	0.0061	0.00234
16	0.1523	0.00425				
17	0.0561	0.00270				
18	0.0252	0.00220				

TABLE II Effective Multiplication Factor and Rossi- $\alpha$  at Delayed Critical obtained from 18-Group Calculations for Experimentally Measured Spherical Critical Assemblies

		Godiva	Topsy	ZPR-III-6F	Jezebel	Popsy
Core	Composition	U(93.8%U-235)	U(94.1%U-235)	14.0%U-235, 31.4%A1 15.9%U-238, 12.3%SS	Pu(4.5%Pu-240)	Pu(1.5%Pu-240)
	Density (cm/cm <sup>3</sup> )	18.75	18.7	7.46	15.66	15.63
Reflector	Composition	-	U(natural)	0.19%U-235, 2.27%A1 83.3%U-238, 7.31%SS	-	U(natural)
	Density (g/cm <sup>3</sup> )	-	18.8	16.5	-	18.8
	Thickness (cm)	-	20.32	~35	-	24.1
Observed Critical Core for Ideal Homog. Sphere	Mass (kg)	52.04 U	17.30 U	133.3 U-235	16.28±0.05 Pu	5.73±0.02 Pu
	Radius (cm)	8.717	6.041	22.97	6.284	4.440
	Volume (l)	2.774	0.9234	50.78	1.040	0.3666
Calculated k <sub>eff</sub>	-	1.004 <sub>5</sub>	1.005	1.006	0.992	1.000
Effective Mean Lifetime $l_{eff}$ (10 <sup>-8</sup> sec)	Exp.	0.60	1.9	7.4±0.4	0.298	-
	Calc.	0.55(0.63)	1.59(1.68 <sub>5</sub> )	6.8 <sub>5</sub> (7.0)	0.30(0.37)	1.25(1.35)
Effective Delayed Neutr. Fraction $\beta_{eff}$ (%)	Exp.	0.66±2%	0.72(estim.)	0.73±0.03(estim.)	0.194±3%	-
	Calc.	0.67±5%	0.70±5%	0.71 <sub>5</sub> ±5%	0.197±5%	0.28±5%
Rossi- $\alpha$ at Delayed Critical (10 <sup>6</sup> sec <sup>-1</sup> )	Exp.	-1.10	-0.37	-0.098 <sub>5</sub> ±0.002	-0.65	-0.20±0.01
	Calc.	-1.22(1.06)	-0.44(0.41 <sub>5</sub> )	-0.104 <sub>5</sub> (0.102)	-0.65 <sub>5</sub> (0.53)	-0.22 <sub>5</sub> (0.20 <sub>5</sub> )

TABLE III Effective Multiplication Factor obtained from  $S_4$  Calculations for Experimentally Measured Critical Enriched U Spheres in Various Reflectors

Material	Reflector				Total Number of Energy-Groups
	Density (g/cm <sup>3</sup> )	Thickness (cm)			
		2.54	5.08	10.06	
Be	1.84	1.002	1.002 <sub>5</sub>	1.002 <sub>5</sub>	6
W Alloy (8 w/o Fe)	17.4	1.007	1.007	1.009	18
Ni	8.88	0.990	0.979	0.984	6
Fe	7.87	0.987 <sub>5</sub>	0.978 <sub>5</sub>	0.988	6
Water	1.00	-	0.979	0.999	6
		-	0.984	1.003 <sub>5</sub>	18
Paraffin ( $N_H = 8.0 \times 10^{22}$ )	0.91	1.009 <sub>5</sub>	-	-	6
		1.010 <sub>5</sub>	-	-	18
WC	14.7	-	1.005	1.001 <sub>5</sub>	18

TABLE IV Effective Multiplication Factor obtained from  $S_4$  Calculations for Experimentally Measured Critical Pu Spheres in Various Reflectors

Core		Reflector					Total Number of Energy-Groups
Density (g/cm <sup>3</sup> )	Pu-240 Content	Material	Density (g/cm <sup>3</sup> )	Thickness (cm)			
				5.22	8.17	13.0	
19.25	3%	Be	1.84	1.023	1.025	1.019 <sub>5</sub>	6
				1.014 <sub>5</sub>	1.016	1.010 <sub>5</sub>	18
15.62	5.21 at %	Be	1.793 <sub>5</sub>	1.003 & 0.996 for thickness 3.688 cm			6 & 18
		W Alloy (9.7 w/o Ni)	17.21	1.022 & 1.020 for thickness 4.699 cm			6 & 18

TABLE V Configurations of Proposed and Realized Mockup Core

	Proposed Core		Realized Core (Nominal Design Pattern)
U-Rod Radius a(cm)	6.35		6.896
Lattice Pitch b(cm)	14.932 <sub>5</sub>		16.30
Composition (vol %)	U	65.60	64.93
	Fe	30.20	34.35
	Void	4.20	0.72
No. of Rods at Core Window n+1	10	9	7+2 <sup>a)</sup>
No. of Rows of Rods 2m+1	9	11	8+1 <sup>b)</sup>
Core Window Width d(cm)	14.301 <sub>5</sub>	12.808	10.721(13.981 <sup>a)</sup> )
Core Width t(cm)	11.839	14.425	-
Total Number of Rods N	106	124	97(-2 <sup>a)</sup> -8 <sup>b)</sup> -2 <sup>c)</sup> = 85 U rods)
Core Area A(cm <sup>2</sup> )	204.69	239.45	195.58
Core Volume V(l)	4.912 <sub>5</sub>	5.747	4.694

a) The rods at the corners are Fe dummies.

b) The 9th row contains only one U rod.

c) The rods at the ends of the 5th row are Fe rods.

TABLE VI Region Specification for the Cylindricalized Representation shown in Fig. 1

Region	Material	Density (g/cm <sup>3</sup> )	Volume Fraction (%)	Note
1 Core	U	18.65 <sub>5</sub>	64.93	93.18% enriched in U-235
	Fe	7.85	34.35 <sub>5</sub>	-
	Void	-	0.72	-
2&3 Dummies	Fe	7.85	100	99.28 vol% Fe in reality
4&6 Extension of Control Rods	Be	1.85	28.01	Control rods #1 & #5 (see Fig. 2)
	Fe	7.85	26.57 <sub>5</sub>	Control rods #2a & #2b
	Void	-	45.41 <sub>5</sub>	-
5 Moving Reflector & Control Rods	Be	1.85	60.69	Moving refl. & control rods #1 & #5
	Fe	7.85	26.57 <sub>5</sub>	Control rods #2a & #2b (see Fig. 2)
	Void	-	12.73 <sub>5</sub>	-
7 Inner Reflector	Fe	7.85	100	-
8 Base Plate	Fe	7.85	100	-
9 Beam Holes	Air	0.0012	100	-
10 Polyethyl. Scatterers	(C <sub>2</sub> H <sub>4</sub> ) <sub>n</sub>	0.93	100	2 scatterers with 11.2 cm $\phi$
11 Outer Reflector	Fe	7.85	100	-
12 Extension of Inner Reflector	Fe	7.85	100	-
13 Scatt. Containers	Al	2.76	53.57	Real composition (thickness in mm);
	B <sub>4</sub> C	1.6	32.14 <sub>5</sub>	from the inside, 2 Al, 2 Void, 5 Al,
	Void	-	14.28 <sub>5</sub>	4.5 B <sub>4</sub> C & 0.5 Al (see Fig. 2)
14 Safety Plug	Fe	7.85	100	Hexagonal cross section in reality

TABLE VII Region Specification for the Horizontal Representation shown in Fig. 2

Region	Material	Density (g/cm <sup>3</sup> )	Volume Fraction (%)	Note
1 Core	(see Table VI)			
3 Core-Window	Fe	7.85	44.44 <sub>5</sub>	Real composition (thickness in mm); from the inside, 5 Fe, 2 Void, 3 Fe, 3 Al & 4+0.5 Void
	Al	2.76	16.66 <sub>5</sub>	
	Void	-	38.89	
4 Reflector	Fe	7.85	100	-
5 Control Rods	Be	1.85	100	Rod #1 on CR side, Rod #5 on S side
6 Moving Refl. Housing	Fe	7.85	100	-
7 Void	Air	0.0012	100	-
8 Moving Reflector	Be	1.85	100	24 cm height
9 Moving Refl. Arm	Fe	7.85	100	-
10 Polyethylene Scatterer	(see Table VI)			Scatterer #3
12 Scatterer Container				
11 Control Rod #2a	Fe	7.85	100	on the control rod side
Polyethylene Scatterer	(see Table VI)			Scatterer #4 on the scatterer side
13 Scatterer Container				
Control Rod #2b	Fe	7.85	100	on the control rod side
15 & 16 Beam Holes	Air	0.0012	100	-
17 Void	Air	0.0012	100	-

TABLE VIII Axial Bucklings ( $\text{cm}^{-2}$ ) to be Adopted for 2DXY Calculations

Region Height (cm) Energy-Group	Core		Fe Station. Reflector	Be Moving Reflector		Polyethylene Scatterer	Scatterer Container
	24	30	48	30	24	48	48
1 10-3 MeV	0.0105	0.0075	0.0075	0.0075	0.0090	0.0090	0.0075
2 3-0.9	0.0100	0.0065	0.0055	0.0055	0.0080	0.0075	0.0070
3 0.9-0.1	0.0085	0.0055	0.0045	0.0045	0.0080	0.0060	0.0055
4 100-0.454 keV	0.0030	0.0030	0.0030	0.0035	0.0065	0.0060	0.0050
5 454-0.414 eV	0.0001	0.0001	0.0030	0.0035	0.0050	0.0060	0.0040
6 0.414 eV -	0.0001	0.0001	0.0030	0.0035	0.0050	0.0060	0.0050
Region Number in Nominal Design shown in Fig. 2	1	-	3,4,6&9 (11&13 on CR side)	5 (48 cm height)	8	10 (11 on S side)	12 (13 on S side)

TABLE IX Calculated Reactivity Worth of Control Rod #2a and the Comparison with the Experimental Value

Between the Core and Rod		1 cm Fe Layer			2 cm Fe Layer			Deviation from Exp.Value (%)
		Calc.Value ( $\rho$ )	Modified by Streaming (+40 $\rho$ )	Exp.Value ( $\rho$ )	Calc.Value ( $\rho$ )	Modified by Streaming (+30 $\rho$ )	Exp.Value ( $\rho$ )	
Material	Density (g/cm <sup>3</sup> )							
Fe	7.85	56 $\pm$ 1	96	80.3	47 $\pm$ 1	77	64.1	+20
W(6% Ni)	17.8	83 $\pm$ 1	123	112.4	65 $\pm$ 1	95	90.0	+ 8
Ni	8.90	70 $\pm$ 1	110	121.4	57 $\pm$ 1	87	98.4	-10
B <sub>4</sub> C	1.65	10 $\pm$ 1	50	55.3	5 $\pm$ 1	35	-	-10

TABLE X Reactivity Worths (Dollars) of Rods inserted in Various Core Positions

Rod Material Density & Diameter ( $\Sigma_a + DB_z^2$ ) for 3rd Group	U(93.18w/o U-235, 6.82w/o U-238)			Mo		Fe		Ti	
	Calcul.	Experim.	Exp.-Cal. = Stream.	Corrected Calcul.	Experim.	Corrected Calcul.	Experim.	Corrected Calcul.	Experim.
	18.65 <sub>5</sub> g/cm <sup>3</sup> , 13.79 mm 0.07674 cm <sup>-1</sup> ( $\nu\Sigma_f = 0.14438$ cm <sup>-1</sup> )			10.2 g/cm <sup>3</sup> , 12.73 mm 0.00692 cm <sup>-1</sup>		7.85 g/cm <sup>3</sup> , 12.70 mm 0.01505 <sub>5</sub> cm <sup>-1</sup>		4.49 g/cm <sup>3</sup> , 12.88 mm 0.01915 cm <sup>-1</sup>	
48	1.515	1.770	0.255	0.125	0.108	-0.029	0.064	-0.116	0.070
71	1.346	1.601	0.255	0.139	0.164	0.004	0.108	-0.074	0.108
45	1.082	1.384	0.302	0.208	-	0.099	0.101	0.034	0.094
51	1.076	1.280	0.204	0.111	0.155	0.002	0.106	-0.060	0.096
25	1.172	1.472	0.300	0.199	0.186	0.082	0.120	0.014	0.096
91	0.736	1.107	0.371	0.308	0.296	0.233	0.205	0.191	0.151
78	0.608	0.984	0.376	0.323	0.266	0.262	0.176	0.227	0.145
43	0.570	0.847	0.277	0.228	0.201	0.170	0.134	0.137	-
53	0.519	0.738	0.219	0.174	0.202	0.122	0.137	0.092	0.104
18	0.451	0.766	0.315	0.276	0.240	0.231	0.163	0.204	0.128
5	0.500	0.886	0.386	0.343	0.291	0.293	0.184	0.264	0.157

TABLE XI Reactivity Worth of the Be Moving Reflector  
as a Function of the Width

Moving Reflector Width (cm)	Calculated Worth (\$)	Measured Worth (\$)
11.0	7.02	6.0 <sub>-</sub> +0.2
16.0	9.72	8.7 <sub>-</sub> +0.2
21.0	11.78	11.0 <sub>-</sub> +0.2
26.2	13.15	12.0 <sub>-</sub> +0.1

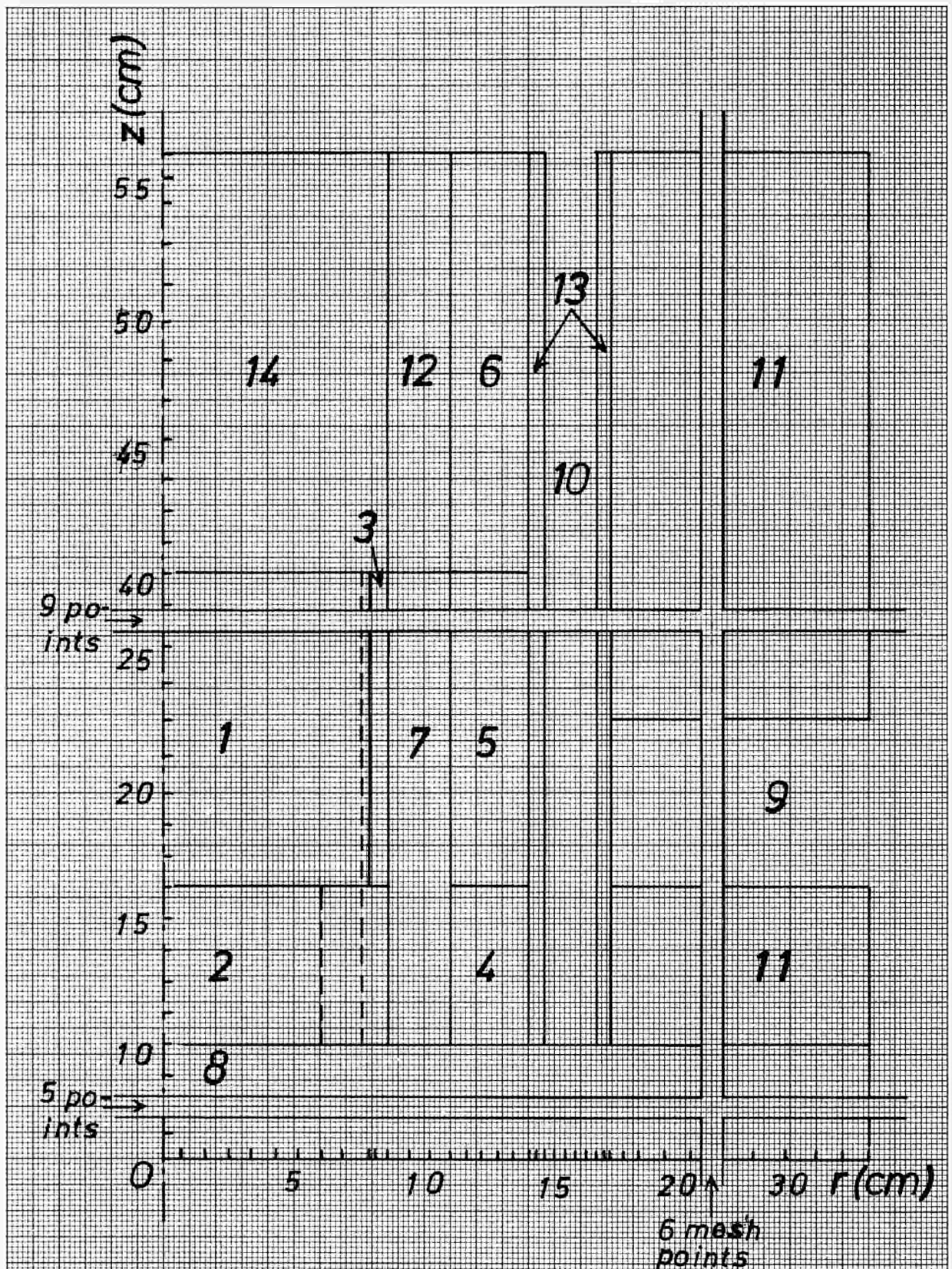


Fig.1 Cylindricalized representation of the mockup with nominal design configuration for TDC calculations

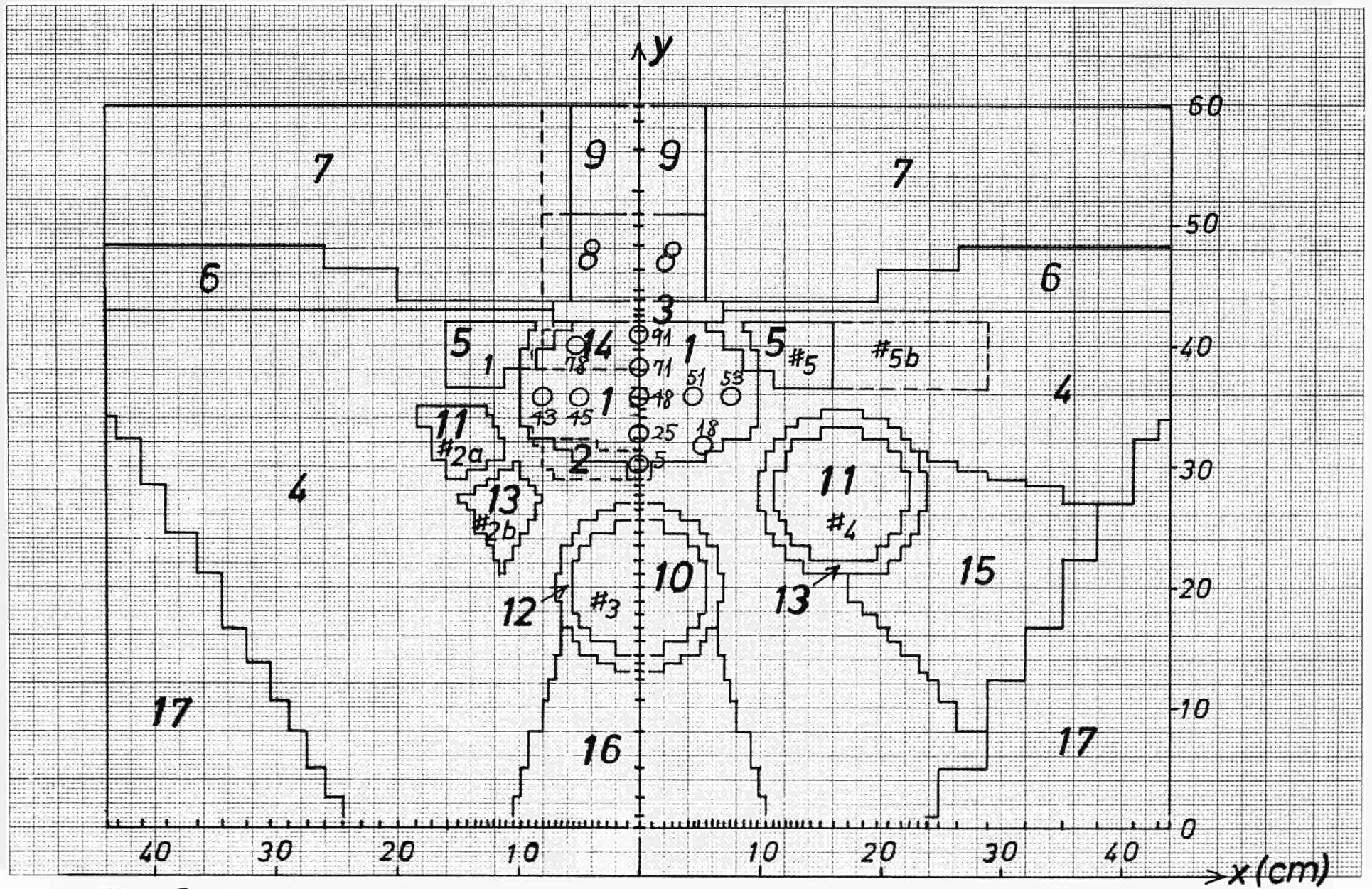


Fig.2 Horizontal representation of the mockup with nominal design configuration for 2DXY calculations

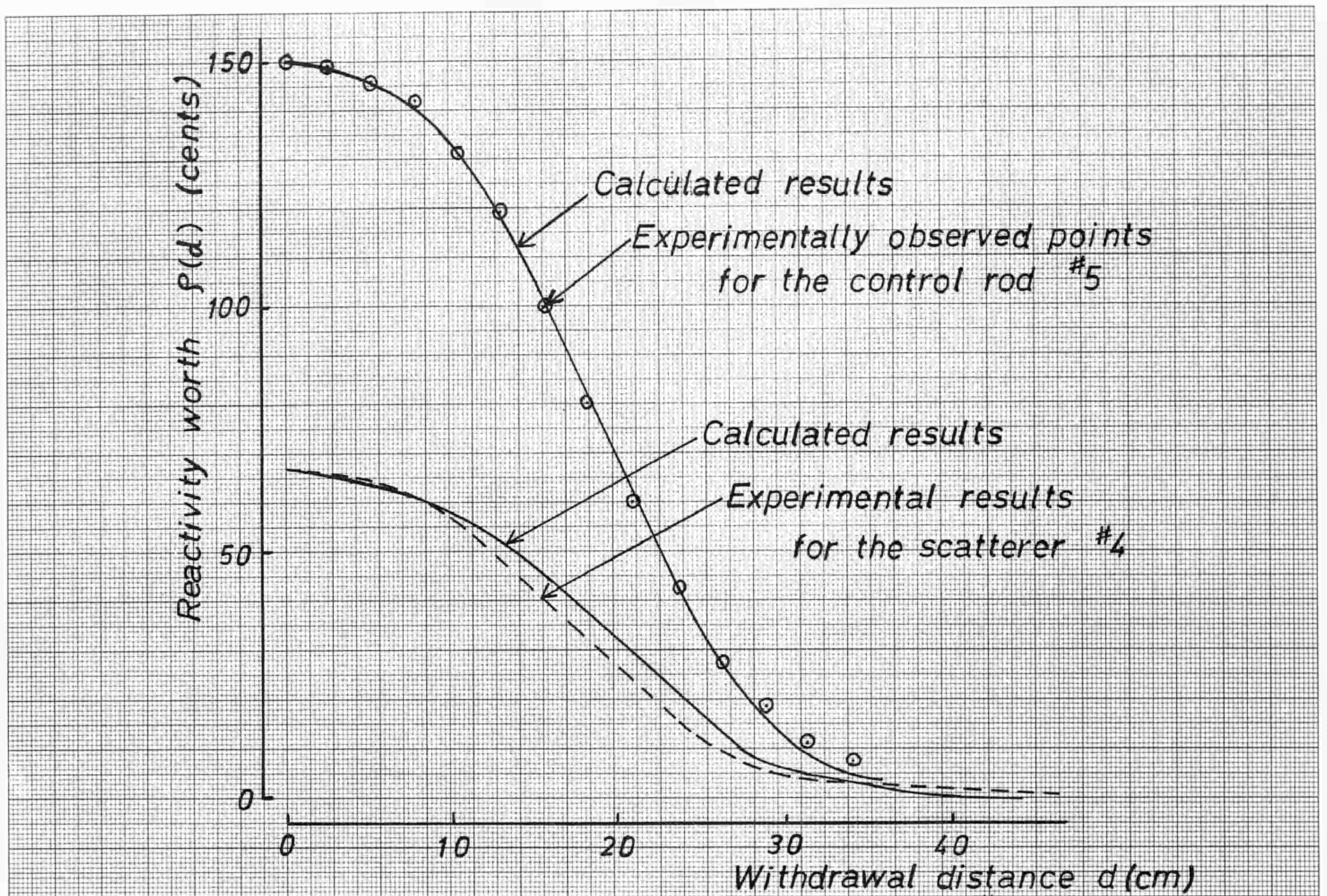


Fig. 3 Reactivity worth of the control rod #5 and the entire scatterer #4 as a function of withdrawal distance

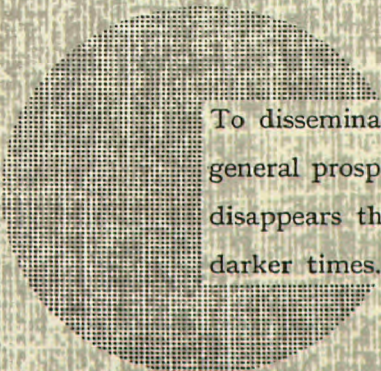
### NOTICE TO THE READER

All scientific and technical reports published by the Commission of the European Communities are announced in the monthly periodical "**euro-abstracts**". For subscription (1 year : US\$ 16.40, £ 6.17, Bfrs 820,-) or free specimen copies please write to :

**Handelsblatt GmbH**  
**"euro-abstracts"**  
**D-4 Düsseldorf 1**  
**Postfach 1102**  
**Germany**

or

**Office for Official Publications**  
**of the European Communities**  
**P.O. Box 1003 - Luxembourg 1**



To disseminate knowledge is to disseminate prosperity — I mean general prosperity and not individual riches — and with prosperity disappears the greater part of the evil which is our heritage from darker times.

Alfred Nobel

## SALES OFFICES

All reports published by the Commission of the European Communities are on sale at the offices listed below, at the prices given on the back of the front cover. When ordering, specify clearly the EUR number and the title of the report which are shown on the front cover.

### OFFICE FOR OFFICIAL PUBLICATIONS OF THE EUROPEAN COMMUNITIES

P.O. Box 1003 - Luxembourg 1  
(Compte chèque postal N° 191-90)

#### BELGIQUE — BELGIË

MONITEUR BELGE  
Rue de Louvain, 40-42 - B-1000 Bruxelles  
BELGISCH STAATSBLAD  
Leuvenseweg 40-42 - B-1000 Brussel

#### LUXEMBOURG

OFFICE DES  
PUBLICATIONS OFFICIELLES DES  
COMMUNAUTÉS EUROPÉENNES  
Case Postale 1003 - Luxembourg 1

#### DEUTSCHLAND

VERLAG BUNDESANZEIGER  
Postfach 108 006 - D-5 Köln 1

#### NEDERLAND

STAATSDRUKKERIJ  
en UITGEVERIJBEDRIJF  
Christoffel Plantijnstraat - Den Haag

#### FRANCE

SERVICE DE VENTE EN FRANCE  
DES PUBLICATIONS DES  
COMMUNAUTÉS EUROPÉENNES  
rue Desaix, 26 - F-75 Paris 15<sup>e</sup>

#### ITALIA

LIBRERIA DELLO STATO  
Piazza G. Verdi, 10 - I-00198 Roma

#### UNITED KINGDOM

H. M. STATIONERY OFFICE  
P.O. Box 569 - London S.E.1

Commission of the  
European Communities  
D.G. XIII - C.I.D.  
29, rue Aldringen  
Luxembourg

CDNA04676ENC